

## Sea level changes at Tenerife Island (NE Tropical Atlantic) since 1927

Marta Marcos,<sup>1</sup> Bernat Puyol,<sup>2</sup> Francisco M. Calafat,<sup>3,4</sup> and Guy Woppelmann<sup>5</sup>

Received 29 May 2013; revised 27 August 2013; accepted 27 August 2013; published 2 October 2013.

[1] Hourly sea level observations measured by five tide gauges at Santa Cruz harbor (Tenerife Island), in the Northeastern Tropical Atlantic, have been merged to build a consistent and almost continuous sea level record starting in 1927. Datum continuity was ensured using high precision leveling information. The time series underwent a detailed quality control in order to remove outliers, time drifts, and datum shifts. The resulting sea level record was then used to describe the low frequency (interannual to decadal) sea level variability at Tenerife. It was found that at interannual and longer time scales, the observed sea level changes are primarily driven by steric sea level variations. Such steric changes are originated by coastal trapped waves induced by longshore winds along the continental coast and propagate poleward. Observed sea level rise at Tenerife was  $2.09 \pm 0.04$  mm/yr since 1927. According to the hydrographic observations in the area, only half of this trend was attributed to steric sea level changes for the top 500 m, at least since 1950.

**Citation:** Marcos, M., B. Puyol, F. M. Calafat, and G. Woppelmann (2013), Sea level changes at Tenerife Island (NE Tropical Atlantic) since 1927, *J. Geophys. Res. Oceans*, 118, 4899–4910, doi:10.1002/jgrc.20377.

### 1. Introduction

[2] Long-term mean sea level changes at time scales of years to decades and centuries display a large spatial variability as a result of the regional distribution of its forcing mechanisms. The description and understanding of this variability is constrained by the uneven geographical coverage of sea level observations and by the limited number of consistent long time series. Only during the last two decades, satellite observations have provided high quality nearly global sea level measurements that have proven extremely powerful. Longer term observations however, are much scarcer; according to the PSMSL data base [Holgate *et al.*, 2013; www.psmsl.org], only around 120 sea level tide gauge records worldwide are longer than 80 years and its geographical distribution is mostly concentrated on the northern hemisphere and along continental shores, which may significantly bias the estimation of global and regional sea level trends and accelerations.

[3] In an attempt to overcome the limitations of the sparse sea level data set, many efforts are presently devoted to the extension of the current historical sea level data base. Wöppelmann *et al.* (2006, 2008) recovered and analyzed

tide gauge observations at Brest dating back to the 18th century from old archives. Other notable exercises of data archaeology can be found in Testut *et al.* [2010], who have provided sea level observations at Saint Paul Island (Indian Ocean) from late 19th century, and Woodworth *et al.* [2010] that linked old sea level measurements from the 19th century with present day observations at Falkland Islands (South Atlantic). Likewise, Watson *et al.* [2010] recovered sparse sea level observations of the 20th century in Macquarie Island (SW Pacific) whereas Marcos *et al.* [2011] built a continuous sea level time series at Cadiz (Southern Spain) after recovering historical tide gauge observations from 1882 to 1924 and linking them with a modern nearby record. More recently, Talke and Jay [2013] described historical sea level measurements in the Pacific and the coasts of North America, starting during the mid-19th century, and identified 600 station years of tabulated data, and Dangendorf *et al.* [2013] used digitized mean sea level observations at Cuxhaven for the period 1871–2008 to study the climatic and meteorological contributions to sea level related to large scale atmospheric forcing.

[4] In 2011, the Global Sea Level Observing System (GLOSS) Group of Experts recognized the potential of tide gauge data rescue and developed a questionnaire aimed at identifying details of archived observations. The responses, compiled and analyzed by Caldwell [2012], revealed that there still exists a huge amount of historical tide gauge measurements in nonelectronic format. A significant part of such data correspond to long time series that could be used in the assessment of long-term sea level rise and changes in extreme high water events [Caldwell, 2012]. The present work represents an example of how the recovery of historical tide gauge data can provide useful information for present-day research on climate in an area poorly sampled such as the Tropical Northeast Atlantic Ocean. The

Additional supporting information may be found in the online version of this article.

<sup>1</sup>IMEDEA, UIB-CSIC, Esporles, Spain.

<sup>2</sup>Instituto Geográfico Nacional, Madrid, Spain.

<sup>3</sup>College of Marine Science, University of South Florida, St. Petersburg, Florida, USA.

<sup>4</sup>National Oceanography Centre, Southampton, UK.

<sup>5</sup>LIENSSE, Université de la Rochelle-CNRS, La Rochelle, France.

Corresponding author: M. Marcos, IMEDEA (UIB-CSIC), Miquel Marquès, 21, ES-07190 Esporles, Spain (marta.marcos@uib.es)

objective of this work is twofold: first, it is aimed at constructing a long and consistent hourly sea level record from the information obtained from log books, nondigitized observations, leveling surveys and modern sea level records at Tenerife Island. Second, it intends to use this new sea level time series to describe the sea level variability at Tenerife Island and to get insight into the underlying processes that drive such variability.

[5] Tenerife Island is part of the Canary Archipelago, located at latitudes  $28^{\circ}$ – $29^{\circ}$ N and about 300 km offshore the African coast (Figure 1). The archipelago is located on the path of the Canary Current, a branch of the Azores Current flowing equatorward along the West African coast up to latitudes  $20^{\circ}$ – $25^{\circ}$ N and driven by the prevailing southerly Trade winds [Navarro-Pérez and Barton, 2001; Hernández-Guerra et al., 2001]. Strong coastal upwelling

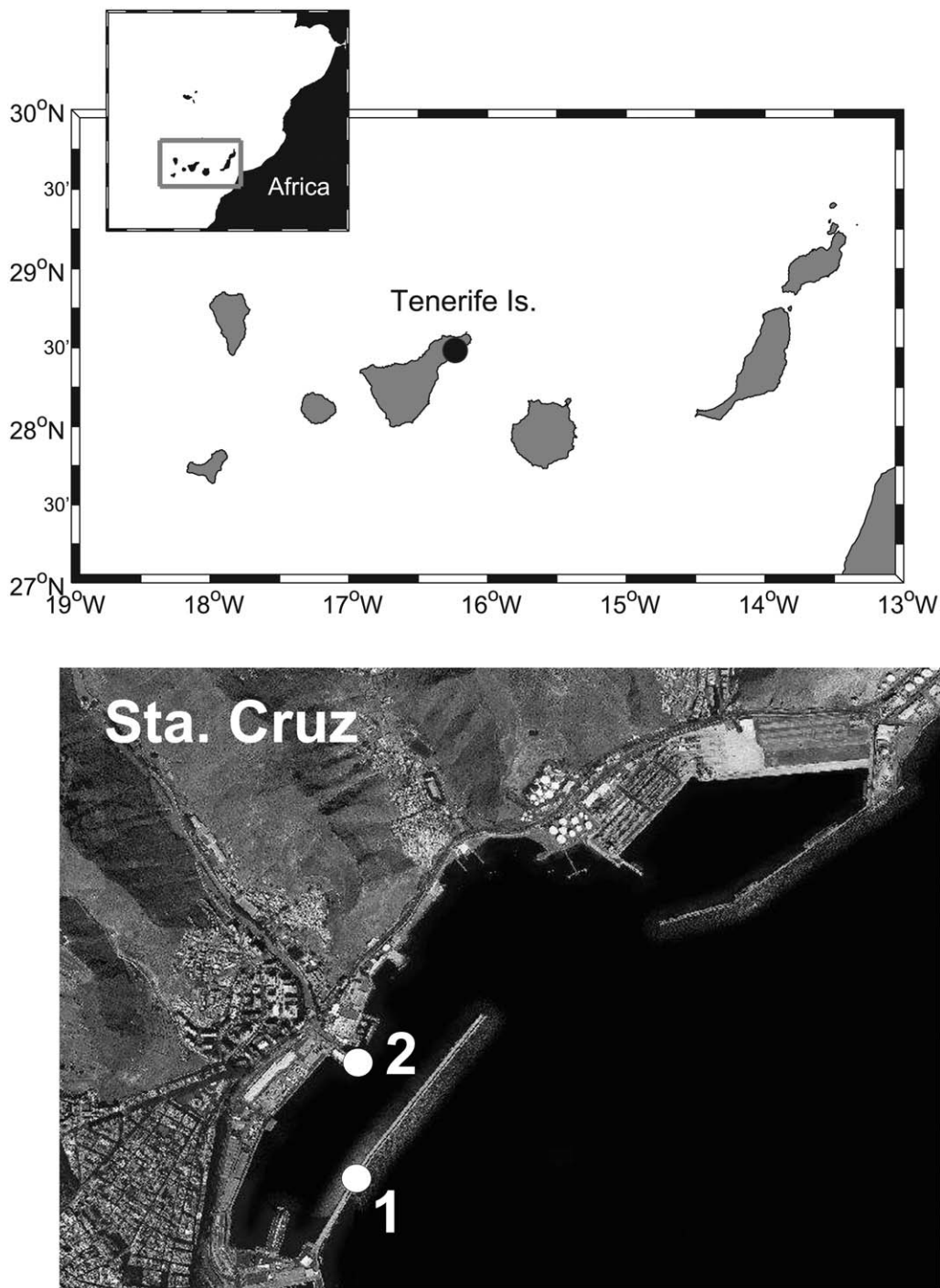


**Figure 1.** (top) Map and location of the Santa Cruz harbor. (bottom) Santa Cruz harbor and sites of the tide gauges: label 1 corresponds to TN011 (southern pier) and label 2 corresponds to TN012 and TN013 (northern pier).

occurs off North West Africa, seasonally and interannually modulated by the wind variability. The bathymetry around Tenerife is steep with a narrow shelf. This makes this location particularly suitable for the study of the sea level changes as it is expected to reflect sea level variability in the deep nearby ocean. Furthermore, its location in a poorly sampled region makes its study even more valuable.

## 2. Tide Gauge Records at Santa Cruz (Tenerife Island)

### 2.1. A Brief Historical Overview

[6] In 1923, the Spanish Geographical Institute (IGN) projected the installation of a tide gauge station at Tenerife Island with the aim of accurately determining the mean sea level at the Canary Islands archipelago. The Spanish engineer Manuel Cifuentes took on the responsibility of defining the best location for the instrument, which was finally established on the southern pier of Santa Cruz harbor (location 1 in Figure 1), under construction by that time. The stilling well was 3.4 m deep and had a diameter of 1.2 m. It was not directly connected to the sea; instead, sea water was filtered in and out through the porous pier due to pressure differences caused by changing water levels. High frequency sea level variations, mostly due to wind waves, were thus filtered out. However, filtering also affected long waves, such as tides, by delaying their timing (without any effect on their amplitude though). The leveling reference of the tide gauge measurements was defined as a benchmark fixed at the well pithead. Two instruments were installed simultaneously on the same well, both recording sea level changes on a continuous tidal chart. The principal was a *Thomson* mechanical floating tide gauge, with a vertical scale factor of 15/100, and the secondary was a *Mier* syphon type tide gauge, whose vertical scale factor was 1/20, thus less accurate. The purpose of this secondary tide gauge was to serve as an additional quality control of the main instrument and, in case of malfunctioning of the *Thomson*, it could also be used to correct/substitute the potential wrong observations. Observations started on 3 January 1927 and both tide gauges were operating until 1936, when measurements were suddenly interrupted due to the Spanish Civil War. In 1940, the observations started over again. Many problems related to the malfunctioning of the *Thomson* tide gauge were reported later on from 1954 until 1956, when measurements were definitely stopped. In 1958, a new location was delivered by the port authority on the northern pier

(location 2 in Figure 1), with a new stilling well of 7 m deep and of 1 m diameter. As in the first case, water was filtered through the pier to reach the well and no direct connection was built with the open sea. This time the reference benchmark was part of the national leveling network (NAPG991, see Table 1 and Figure 2). The two tide gauges were then moved to the new location. However, since the beginning, many problems were reported with the *Thomson* tide gauge, likely attributed to the substitution of the perforated tape connecting the pulley with the floating device, originally metallic, by one made of nylon. Log books document continuous drifts of the measurements which obliged to recalibrate the instrument every few days. In 1965, the perforated tape, the floating device and the pulley were all replaced, and the instrument operated properly since then. The scale factor was changed to 1/10. The *Mier* instrument continued operating until 1975. In 1990, the port authority changed the location of the tide gauge station to a new well, very close to the former (location 2 in Figure 1), on the northern pier. The *Thomson* tide gauge was substituted by an *AOTT* tide gauge, with a vertical scale factor of 1/5 and was referenced to the leveling benchmark NAPH413 (Table 1 and Figure 2). Sea level observations of the new tide gauge started in 1991; however, very soon it was found out that the new well often suffered from obstruction problems. These were solved in 1993 and the reference benchmark was subsequently changed to the new NGU320 (Table 1 and Figure 2). The tide gauge has since then been working. A digital encoder was installed in 1997, providing sea level measurements with a time interval of 10 min in a digital format. In 2007, a new radar *Vega* tide gauge was installed on the same pier with a sampling interval of 5 min (1 min since November 2008). In parallel, the Spanish Port Authority installed an acoustic *SONAR* tide gauge in 1992 nearby the location of the TN013 floating tide gauge (PdE in Figure 1). This was part of the national tide gauge network operated and maintained by the Spanish Port Authority (PdE, www.puertos.es). It provided 5 min sea level observations with respect to the benchmark SS412 (Table 1 and Figure 2). In 2009, the same agency substituted the acoustic tide gauge by a radar *MIROS* tide gauge, which is still in operation.

### 2.2. Sea Level Observations

[7] Sea level observations were obtained from five tide gauge records located at Santa Cruz harbor (Tenerife Island) that operated at distances less than 500 m from each other. The characteristics and periods of operation of the instruments, outlined in the previous section, are summarized in

**Table 1.** Characteristics of the Tide Gauge Records

| Tide Gauge Record | Agency | Manufacturer                         | Period of Operation | Sampling                         | Benchmark                                  |
|-------------------|--------|--------------------------------------|---------------------|----------------------------------|--|
| TN011             | IGN    | Thomson                              | 1927–1956           | Hourly                           | Inner BM                                   |
| TN012             | IGN    | Thomson                              | 1958–1990           | Hourly                           | NAPG991                                    |
| TN013             | IGN    | AOTT                                 | 1992–ongoing        | Hourly (<1997)<br>10 min (>1997) | NAPH413(<1993)<br>NGU320(>1993)            |
| Secondary         | IGN    | Mier                                 | 1927–1975           | Hourly                           | Same as primary tide gauge for each period |
| Secondary         | IGN    | Vega                                 | 2007–ongoing        | 5 min (<Nov/2008)<br>1 min       | NGU320                                     |
| PdE               | PdE    | SONAR (1992–2009)<br>Miros (>5/2009) | 1992–ongoing        | 5 min                            | SS412                                      |

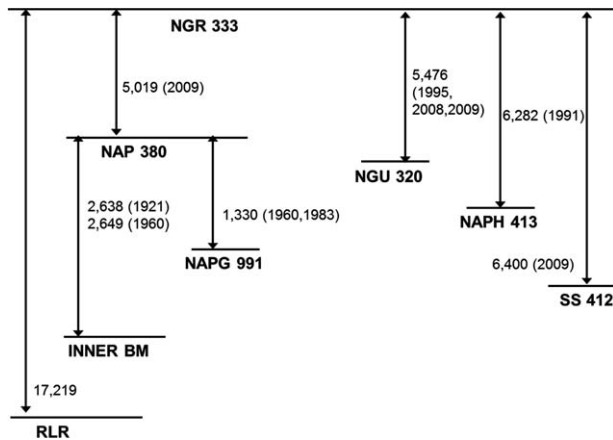


**Figure 2.** Relative heights (in m) between benchmarks. See Table 1 for the correspondence to tide gauges. Years of each leveling survey are indicated in parenthesis.

Table 1 (data from the secondary *Vega* tide gauge was not used in this study). TN011, TN012, and TN013 refer hereinafter to the observations of the primary tide gauge. Hourly sea level data of TN011 and TN012 (i.e., from 1927 to 1990) corresponded to hand-written observations obtained from the tidal charts and stored in log books that have been archived at the Spanish National Geographic Institute (IGN) in Madrid. All these observations were digitized and converted into electronic format. The same applies to observations of TN013 until 1997. After then, sea level observations were acquired as a digital output with a temporal sampling of 10 min. The PdE tide gauge has provided sea level measurements every 5 min since 1992 in a digital format. This time series has been used as an additional quality control of the TN013 time series and to fill in data gaps when needed. Additionally, a few years of digitized data of the secondary *Mier* tide gauge (1955–1957 and 1958–1965) were also available and were used to quality control. Five different benchmarks were used since 1927, as indicated in Table 1. The relationships among benchmarks are discussed below.

### 2.3. Data Calibration and Datum Continuity

[8] Until 1997, sea level observations of the floating gauges (records TN011, TN012, and TN013) were provided as noncalibrated data. The information needed to convert these noncalibrated tidal chart readings into actual sea level values with respect to a given benchmark is referred to as the “tide gauge constant.” This parameter measures the difference between noncalibrated values and the actual distance of sea level to the benchmark and, in absence of technical problems, it should remain unchanged, as its name suggests. Variations of this parameter indicate vertical movements with respect to the tide gauge benchmark which can be attributed to changes in the tide gauge reference, for instance if all or part of the tide gauge has changed position for maintenance, but also to recalibration of the instrument due to malfunctioning. The “tide gauge constants” were provided daily or half-daily for TN011 and TN012 records (1927–1990). A simple visual examination of the “tide gauge constants” time series revealed that the series was not always stable. In particular, for the period 1958–1964, the series was far from homogeneous

and presented a clear seesaw shape. This was certainly related to the malfunctioning problems detected after the change to TN012 location and reported in the historical documentation. For the entire period of TN011 and TN012, 1927–1990, raw observations were calibrated on the basis of hourly interpolated “tide gauge constants.”

[9] The secondary *Mier* tide gauge observations, for which the “tide gauge constants” were provided on a daily basis, were also calibrated as described above for the primary TN011 and TN012 records.

[10] For TN013 record, only values for 1993 unevenly distributed (8–10 values per month) were provided. The averaged “tide gauge constant” was computed for the available period, after discarding outliers greater or lower than the standard deviation of the total series of constants. The obtained mean parameter was used to calibrate all observations for the period 1992–1997.

[11] Calibrated sea level observations of TN011, TN012, and TN013 were referred to four different benchmarks (Table 1). High precision leveling information was used to link the benchmarks with the aim of building a single sea level time series with datum continuity. A total of 10 leveling surveys were carried out in the vicinity of the tide gauges between 1921 and 2010. The resulting heights were carefully checked to detect eventual shifts between two subsequent surveys and to identify the most stable benchmarks. For all cases examined, the closure errors of the leveling surveys were smaller than 2 mm at each path, ensuring thus the reliability of the results. It was found that all benchmarks used to link the tide gauge references were stable, except for the inner benchmark used at TN011 record. In this case, two surveys performed in 1921 and 1960 detected a shift with respect to the benchmark NAP380 of 11 mm, or equivalently 0.27 mm/yr of subsidence if we assume that the change is linear. This correction was therefore applied in the form of a linear trend to the TN011 record. The relative heights between benchmarks are schematically shown in Figure 2. All sea level observations from the three records TN011, TN012, and TN013 were referred to the common datum NGR333, which was considered as the most adequate due to its stability and location close to the modern tide gauge. This benchmark is part of the high precision Spanish national leveling network. The result was a consistent hourly sea level record for the period 1927–2012; this is the sea level time series that will be used hereinafter for the subsequent analysis. In addition, the *Mier* secondary and the PdE time series were also referred to the same benchmark, in order to be used as complementary data to the main longest record.

### 2.4. Quality Control and Tidal Analysis

[12] Hourly values larger or lower than three times the standard deviation of the total time series were considered as outliers and were consequently removed. Smaller but persistent outliers were also observed during the period 1958–1964, which were consequence of the recalibration procedures as described above. Little can be done to improve these data, except to substitute them with the secondary tide gauge observations. We decided to substitute the primary *Thomson* sea level observations with those from the less accurate but well calibrated *Mier* tide gauge for the period January 1958 to December 1964. In 1955–1956, a

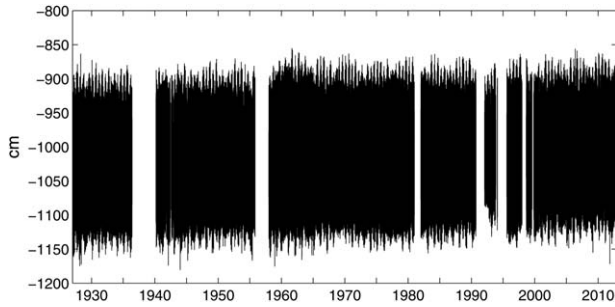


**Figure 3.** Hourly sea level time series referred to the NGR333 benchmark.

datum shift was also observed (not shown) which was not documented in the log books. In this case, the *Mier* data presented a similar problem than the primary record and could not be used to correct it. Therefore, in absence of any other information, the period November 1955 to December 1956 was removed. The resulting hourly sea level time series, after these first corrections were applied and referred to the NGR333 benchmark, is plotted in Figure 3. In the following, a more detailed and careful quality control based on tidal analysis is performed.

[13] A tidal analysis was applied for the period 1965–1977. This time interval was identified as the continuous most stable longest period and was therefore used to estimate the most reliable tidal constituents for the study site. The tidal analysis was performed using the *t\_tide* software package [Pawlowicz *et al.*, 2002] and only those tidal constituents, among the initial 143, with a signal-to-noise ratio larger than 2 were considered. The estimated tidal amplitudes of the major constituents (i.e., those with amplitudes larger than 1 cm) are listed in Table 2, together with their corresponding confidence intervals. Annual and semiannual cycles were removed as their origin is mostly nonastronomical. The estimated tidal phases have not been listed because they depend on the delay induced by the water filtering inside the well and are thus not representative of the actual tidal phases at Tenerife. Results indicated that Tenerife has a semidiurnal tidal regime, with tidal oscillations between  $\pm 1.5$  m and with M2 being the largest constituent (72 cm).

**Table 2.** Major Tidal Constituents (With Amplitudes Larger Than 1 cm) at Tenerife

| Tidal Constituent | Frequency (hours) | Amplitude (cm)   |
|-------------------|-------------------|------------------|
| Q1                | 26.87             | $1.37 \pm 0.04$  |
| O1                | 25.82             | $4.40 \pm 0.04$  |
| P1                | 24.07             | $2.09 \pm 0.05$  |
| K1                | 23.93             | $5.89 \pm 0.05$  |
| 2N2               | 12.91             | $2.10 \pm 0.05$  |
| MU2               | 12.87             | $2.94 \pm 0.05$  |
| N2                | 12.66             | $15.06 \pm 0.05$ |
| NU2               | 12.63             | $2.83 \pm 0.05$  |
| M2                | 12.42             | $72.57 \pm 0.05$ |
| L2                | 12.19             | $2.25 \pm 0.07$  |
| T2                | 12.02             | $1.63 \pm 0.05$  |
| S2                | 12.00             | $27.40 \pm 0.05$ |
| K2                | 11.97             | $6.76 \pm 0.04$  |

[14] All the tidal constituents estimated using the reference period were used to build an hourly tidal time series for the entire length of the record (1927–2012). The objective was to identify periods with time drifts or shifts, potential changes in the reference time and malfunctioning of the instrument. To do so, a detailed comparison between tidal predictions and observations was done by computing lag correlations between the two time series on a monthly basis. Since the time lags between both series were expected to be smaller than the sampling period (1h), the time series were first linearly interpolated to 1 min time interval. Lag correlations were then computed for each calendar month and the time lag of maximum correlation was identified. The resulting time lags of maximum correlation are represented in Figure 4. The largest time lags, with values up to 100 min, were found for the years 1992–1994, during which sea level oscillations appeared anomalously smaller than average (see Figure 3). This result suggested malfunctioning of the instrument due to an obstruction of the stilling well which induces variations of the tidal amplitudes and phases [e.g., Agnew, 1986; Pugh, 1987]. It is thus in agreement with the reported problems in the log books. These years were consequently removed from the record. Instead, hourly sea level observations of the PdE tide gauge (that were referred to the same common benchmark) were used to fill in these data gaps. Additionally, for the entire common period, starting in July 1992, both time series were compared and PdE was used to fill in data gaps of the original series whenever possible.

[15] During the period 1958–1964, it was found a time lag of 1 h, suggesting a shift of the internal clock starting in 1965. Unfortunately, no historical documentation could be found confirming this hypothesis. This period was corrected simply by advancing the timing 1 h. Finally, the record corresponding to TN011 (1927–1956) appeared to be in advance by an average of 36 min with respect to the current timing. The likely explanation for this discrepancy is that the delay induced by water filtering through the pier was different at the well locations of TN011 and TN012. This effect does not affect the quality of the observations and was thus not corrected.

### 3. Other Data Sets and Methodology

[16] In order to investigate the observed sea level variations at Tenerife and its forcing mechanisms, the data sets listed below were used as complementary data.

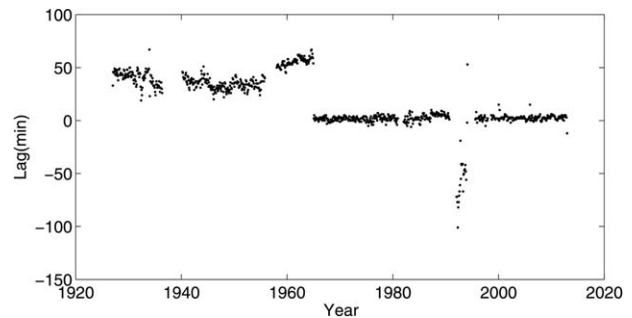


**Figure 4.** Lags of maximum correlation between observations and tidal predictions computed for each calendar month.

[17] Monthly gridded mean sea level pressure and wind stress fields were obtained from the 20th century Reanalysis data set [Compo *et al.*, 2011], with a grid spacing of  $2^\circ \times 2^\circ$  and spanning the period 1871–2010. These data sets were used to quantify the local response of sea level to atmospheric pressure and wind. Atmospheric pressure fields were used to quantify the inverted barometer (IB) contribution to sea level as:

$$IB = \frac{1}{g\rho_0}(\bar{P}_a - P_a). \quad (1)$$

where  $P_a$  is the atmospheric pressure,  $g$  the gravity acceleration, the bar denotes averaging over the global oceans, and  $\rho_0$  is the reference water density.

[18] Besides the barotropic response of local atmospheric pressure and winds, Calafat *et al.* [2012] proved that coastal sea level variations on the eastern boundary of the North Atlantic northward of about  $25^\circ\text{N}$  display a baroclinic response to longshore winds. In essence, when the wind blows parallel to the coast with the coast on its left it displaces surface water offshore through Ekman transport. Because there can be no flow normal to the coast, the displaced surface water needs to be replaced by denser water from deeper levels, which pushes the thermocline upward and thus results in a decrease in the steric sea level. This effect, however, is not purely local because the induced changes in the thermocline can propagate poleward along the coast in the form of boundary waves affecting a large portion of the coast northward of the region of forcing [Gill, 1982]. Following Calafat *et al.* [2012], the response to the longshore wind was quantified using the expression:

$$\int_{y_0}^y \tau^s \left( y', t - \frac{y - y'}{c} \right) dy'. \quad (2)$$

where  $c$  is the internal wave velocity (1–3 m/s),  $\tau^s$  is the wind stress parallel to the coast,  $y_0$  is the zero latitude and  $y = 28^\circ\text{N}$  corresponds to the latitude of Tenerife. For the integration, we used the International Comprehensive Ocean-Atmosphere Data Set (ICOADS) (<http://www.esrl.noaa.gov/psd/>) wind data as they provide actual ground measurements of wind with a relatively good coverage of the African continental shelf at the latitudes of interest. This data set consists of monthly mean wind observations on a global  $2^\circ \times 2^\circ$  grid spanning the period 1800 to present. In order to obtain a continuous time series of the integrated longshore wind, wind data during months in which wind observations are not available are obtained from the 20th century reanalysis [Compo *et al.*, 2011].

[19] Other sea level data sets were also included in the analysis in order to investigate the regional sea level coherence. Monthly gridded mean sea level anomalies with a map spacing of  $1/4^\circ \times 1/4^\circ$  were downloaded from AVISO data server ([www.aviso.oceanobs.com](http://www.aviso.oceanobs.com)). These data consists of a multisatellite global product, which combines up to four altimetric satellites and spans the period from October 1992 to present. All geophysical corrections were applied, including the so-called dynamic atmospheric correction (DAC) [Volkov *et al.*, 2007]. DAC consists of a combination of a barotropic model forced by winds and atmospheric

pressure for periods shorter than 20 days and the inverted barometer (IB) correction for longer periods.

[20] In addition to altimetric observations, other tide gauge records were also considered. Monthly mean sea level tide gauge time series at Cascais, Santander, Brest, and Newlyn were downloaded from the Permanent Service for Mean Sea Level (PSMSL) data repository ([www.psml.org](http://www.psml.org)). All records considered are Revised Local Reference (RLR), that is, they have been checked and corrected for local datum continuity over time relative to benchmarks in the vicinity [Holgate *et al.*, 2013].

[21] The contribution of density changes to sea level at Tenerife was investigated using hydrographic observations. Ocean temperature (T) and salinity (S) profile data were obtained from the EN3 dataset in its version v2a [Ingleby and Huddleston, 2007] available at the Met Office Hadley Centre (<http://www.metoffice.gov.uk/hadobs/en3/>) for the period 1950–2011 and located within the area  $24\text{--}32^\circ\text{N}$  and  $20\text{--}14^\circ\text{W}$ . The profiles version with time varying XBT corrections [Wijffels *et al.*, 2008] was selected. T and S profiles that did not pass the quality controls were discarded for the analysis. For each calendar month of the entire period 1950–2011, the corresponding T and S profiles were first interpolated onto the same depths from 10 to 500 m at 10 m depth intervals and were afterward averaged out in order to build a single monthly profile, whenever possible. Standard deviations for each depth were also computed.

[22] Additionally, hydrographic observations from the RAPROCAN program (<http://www.oceanografia.es/raprocan/>) were kindly provided by the Spanish Institute of Oceanography. The data belong to a monitoring program of the deep ocean around the Canary Islands and consists of a hydrographic section at  $29.5^\circ\text{N}$  and between  $13$  and  $24^\circ\text{W}$  carried out twice a year. Data are available for only a few surveys in 1997, 1998, and from 2004 onward. T and S profiles are measured at 30 hydrographic stations down to the bottom and at 1 m depth intervals. This data set has been carefully edited, calibrated, and quality controlled. RAPROCAN data lying within the target area were processed in the same way as described above for EN3 profiles and were integrated in the analysis.

[23] T and S profiles were used to compute the steric sea level by integrating down to a predefined reference pressure (Pref) the specific volume anomalies ( $\alpha$ ):

$$Steric = \frac{1}{g} \int_{Pref}^0 \alpha(T, S) dp. \quad (3)$$

#### 4. Long-Term (Monthly to Decadal) Sea Level Variability at Tenerife

[24] Quality controlled hourly observations were used to compute monthly mean sea level. Only those months with at least 50% of valid observations were considered. The resulting monthly time series is plotted in Figure 5 (left plot, black line). The monthly time series is available as supporting information. The most prominent signal in the monthly time series is the seasonal cycle. The mean amplitudes and phases of the annual and semiannual signals were

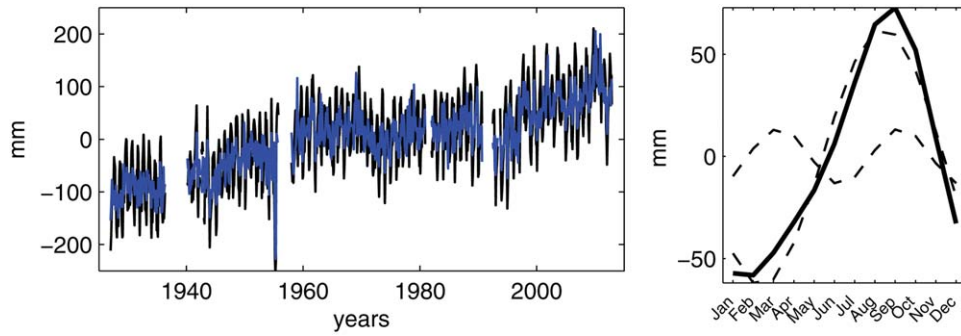


**Figure 5.** (left) Monthly mean sea level with (black) and without (blue) seasonal cycle. (right) Mean annual and semiannual cycles (dashed lines) and mean seasonal cycle (solid line).

estimated using least square fitting of two sinusoidal signals. It was found that the seasonal cycle accounts for 34% of the total monthly sea level variance. The mean annual and semiannual amplitudes obtained were 6.3 cm and 1.3 cm, the first peaking in August and the second in February (Figure 5, right plot). The monthly deseasoned sea level record is plotted in Figure 5 (blue line). Despite having removed the mean seasonal cycle, there is still residual energy evident at the annual frequency. The reason is that the seasonal cycle varies both in space and time [Marcos and Tsimplis, 2007; Barbosa et al., 2008]. Therefore, its temporal variability was explored by estimating the annual and the semiannual signals for 5 year periods, overlapping year-to-year. The resulting changes in the annual and semiannual amplitudes, together with their standard errors, are plotted in Figure 6 (top). The standard deviations are 1 cm and 0.5 cm for the annual and semiannual amplitudes, respectively. Annual amplitudes change up to 3 cm within the observation period, with smaller values between 1960s and 1980s. A look at the seasonal winter and summer averages (Figure 6, bottom) indicates that the decrease in the annual cycle amplitudes was due to higher than average winter sea levels, while summer sea levels displayed smaller interannual variability.

#### 4.1. The Contribution of Local Atmospheric Pressure and Wind

[25] The barotropic response of sea level to the combined effect of atmospheric pressure and wind is nowadays

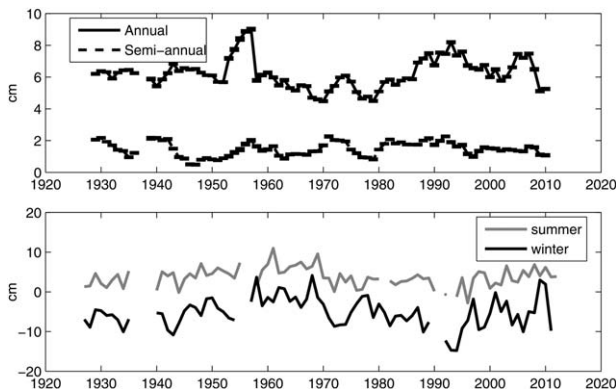


**Figure 6.** (top) Temporal variability of the annual and semiannual amplitudes of the seasonal cycle, computed for 5 years period overlapping year-to-year. (bottom) Seasonal winter (DJF) and summer (JJA) sea level averages.

routinely calculated using vertically integrated ocean models. However, only rarely this barotropic component is available for a long-term period. Unfortunately, there is not, to our knowledge, such kind of information for the area of the Canary Islands for the last decades; therefore, the barotropic component of sea level at Tenerife was quantified using an empirical relationship between mean sea level and atmospheric pressure and wind stress fields. The closest grid points of mean sea level pressure and wind stress from the 20th Century Reanalysis data to the tide gauge were chosen as representative of the forcing fields at its location. To ensure global ocean mass conservation, the averaged sea level pressure over the global oceans (which is time-varying in general) was subtracted from the local sea level pressure time series at Tenerife. We must remark that the steep orography of Tenerife Island partly determines the local winds of the island. Hence, the atmospheric re-analysis has a too coarse spatial resolution to capture such local features. Therefore, the barotropic contribution determined with an empirical relationship will likely miss this local variability.

[26] A multiple regression was applied using atmospheric pressure and zonal and meridional wind stress time series as predictors for the common period:

$$Sea\ Level = aP + bWindStressX + cWindStressY$$

[27] All time series were detrended and deseasoned prior to the analysis. The regression coefficients  $a$ ,  $b$ , and  $c$  were obtained using least squares. Our intention was to keep the long-term contributions of atmospheric pressure and wind to the barotropic term; to do so, we have used deseasoned, but not detrended, forcing fields when the barotropic component was estimated based on the coefficients  $a$ ,  $b$ , and  $c$ .

[28] The regression coefficients for Tenerife sea level record resulted in  $a = -0.58\text{ cm/mbar}$ ,  $b = 43.77\text{ cm/(N/m}^2\text{)}$  and  $c = -20.18\text{ cm/(N/m}^2\text{)}$ . The overall variance reduction in monthly sea level accounted for by the barotropic contribution was 9%, according to this regression model. If only atmospheric pressure is considered the variance reduction decreases to 5%. The monthly mean sea level time series (deseasoned) and the predicted barotropic contribution at Tenerife are plotted in Figure 7. The most significant difference between the two time series is the sea level rise observed in total sea level, which is attributed to causes other than the direct atmospheric forcing. The linear sea level trend estimated from monthly deseasoned observations

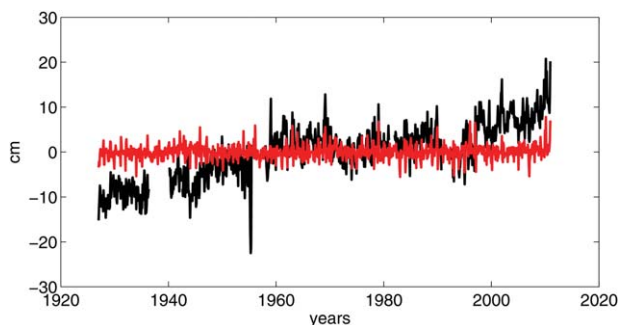


**Figure 7.** Monthly mean sea level (black) and the barotropic contribution obtained from the multiple regression model (red). Both time series are deseasoned.

was  $2.07 \pm 0.05$  mm/yr (uncertainties quoted correspond hereinafter to standard errors) for the entire period 1927–2010, whereas when the barotropic contribution was removed it became  $2.04 \pm 0.04$  mm/yr. This is consistent with the barotropic component having an overall trend of  $0.04 \pm 0.02$  mm/yr. Seasonal differences in the long-term barotropic contribution were found to be slightly higher during autumn and winter (0.06 mm/yr) than during spring and summer ( $-0.01$  and 0.03 mm/yr, respectively).

#### 4.2. Interannual and Decadal Sea Level Variations

[29] After removing the barotropic sea level component, the residual mean sea level changes display large decadal sea level variability, as suggested by Figure 7. The mechanisms driving decadal sea level variability along the western European coasts were recently explored by *Calafat et al.* [2012]. They found that, at decadal time scales, sea level fluctuations are highly correlated along the western European coast and provided evidence that the observed sea level variability was linked to the poleward propagation of wind-driven steric sea level fluctuations along the coast. Thus, other mechanisms influencing decadal sea level variability, such as local surface heat fluxes, and mass redistribution in the north Atlantic linked to changes in the strength of the subtropical gyre, were discarded. They proved so for tide gauges at latitudes higher than  $40^\circ\text{N}$ , whereas *Sturges and Douglas* [2011] demonstrated the same relationship at Cascais ( $39^\circ\text{N}$ ). *Calafat et al.* [2012] suggested, on the basis of the output of a numerical model, that the correlation between longshore wind effects and sea level at decadal scales may also hold at latitudes as low as  $28^\circ\text{N}$ . We therefore compared decadal sea level at Tenerife with longshore winds. Following *Calafat et al.* [2012], the effect of wave-propagation is accounted for by integrating the longshore wind from the equator up to the latitude of Tenerife ( $\sim 28^\circ\text{N}$ ; equation (2)). The resulting time series of the integrated longshore wind, detrended and smoothed with a 2 years running mean, are compared with the sea level (corrected for local atmospheric and wind effects) from the tide gauge record at Tenerife in Figure 8. Note that the integrated longshore wind as calculated here provides an estimate of the variability of the sea level response to the longshore wind but not the right magnitude [*Calafat et al.*, 2012]; thus it was rescaled for comparison with observed sea level. The correlation between these two series was 0.6 (significant at the 95% confidence level), and this in spite

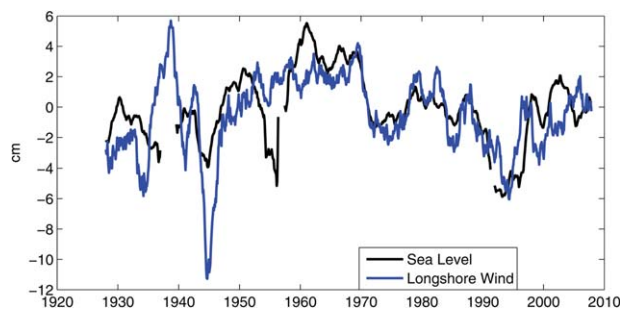


**Figure 8.** Detrended and smoothed with a 2 year running mean sea level at Tenerife (black) and integrated longshore wind at  $28^\circ\text{N}$ .

of the exceptionally large longshore wind variations around 1940. Such longshore wind changes are not realistic and are due to the uneven distribution of wind observations over the ocean and the lack of data, especially during the World War II. When only the period from 1958 onward was considered, the correlation increased to 0.8. Lag correlations indicated that the longshore wind contribution appeared to be 1 month in advance with respect to the sea level at Tenerife. This is in agreement with *Calafat et al.* [2012] and *Sturges and Douglas* [2011], despite their records were all along continental shores.

[30] Changes in steric sea level associated with longshore wind forcing of the thermocline are dominant at decadal scales, but nothing can be said about its longer term contribution due to the limitations of the wind observations. For this reason, the steric contribution (equation (3)) to long-term sea level trend has been explored using hydrographic data. The resulting monthly averaged T and S profile time series are plotted in Figure 9. Hydrographic observations around Tenerife revealed a deepening of the thermocline during the last four decades and heating of the upper waters (down to 100 m). Likewise, although very scarce, S observations suggested significant S increases during the years 2000s with respect to the 1970s (this is reflected in the deepening of the isohalines). It is worth mentioning that the same effect of rising mean T and salinification of the upper waters can also be detected in the RAPROCAN observations. We thus consider that this result is robust.

[31] Steric sea level was computed for each monthly averaged profile of T and S fully covering the top 500 m following equation (2). Though this is a restrictive criterion, it is the only way to ensure consistency among all steric values. The reference level of 500 m was chosen as a compromise between the number of profiles available and their representativeness of the steric changes. After deseasoning, the resulting steric sea level was compared with observed sea level at the tide gauge with the barotropic correction applied (Figure 10). The correlation between the two time series, although statistically significant, was low (0.22) at interannual time scales. However, the correspondence at longer periods was much better. When a 12 months running average was applied to both time series (not shown), the correlation became 0.43, despite the number of observations was significantly reduced due to the discontinuities in the steric record. Likewise, steric sea level was correlated with the longshore wind contribution



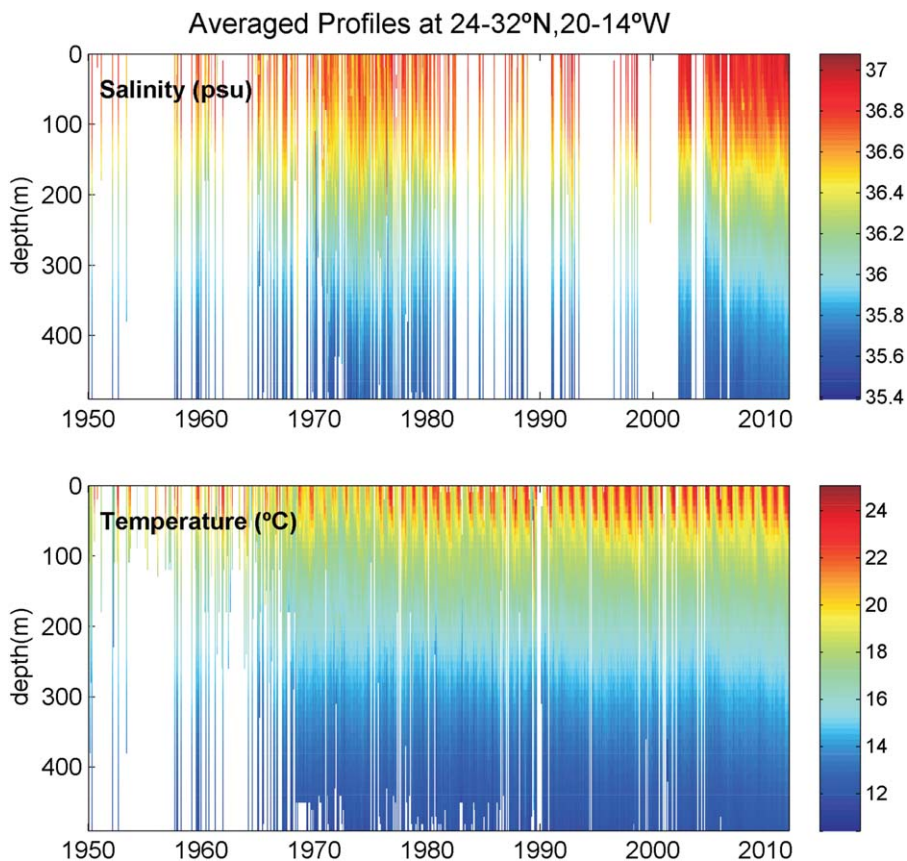


**Figure 9.** Temperature and salinity monthly averaged profiles for the top 500 m in an area surrounding Tenerife.

with a value of 0.54 (after the running average was applied), as expected. For the common period 1950–2011 the atmospherically corrected sea level trend was  $1.48 \pm 0.07$  mm/yr, while the steric sea level trend was  $0.76 \pm 0.09$  mm/yr. If only the period 1970 onward was selected, the linear trends were  $2.22 \pm 0.10$  mm/yr and  $1.16 \pm 0.10$  mm/yr for the atmospherically corrected tide gauge and steric sea level, respectively. The differences in trends arise due to the enhanced sea level rise shown by the

tide gauge during years 2000s, rather than due to the lack of steric data.

### 5. Regional Sea Level Coherency

[32] The regional coherency of sea level changes at Tenerife was investigated using altimetric observations and tide gauges located along the European coasts. Linear correlations between deseasoned and detrended sea level at Tenerife and sea level anomalies from satellite altimetry for the period 1992–2011 are mapped in Figure 11. The IB correction (equation (1)) was applied to the tide gauge record in order to be consistent with satellite altimetry data. The correlations with other tide gauges at Cascais, Santander, Brest and Newlyn, for their common periods are also mapped (all of them were IB corrected). Higher correlations (0.65) were found between the tide gauge record at Tenerife and satellite altimetry in the vicinity of the Canary Islands, as expected. Interestingly, correlations as large as 0.4–0.5 were also found over the continental shelf along the African and European coasts from around 26°N up to latitudes as high as 50°N. The correlations obtained between tide gauges, although lower than for the altimetric period (0.2–0.3), were also significant. This coherent signal along the continental coast was consistent with a response of sea level to the integrated longshore winds along the coast, as has already been identified for decadal time scales

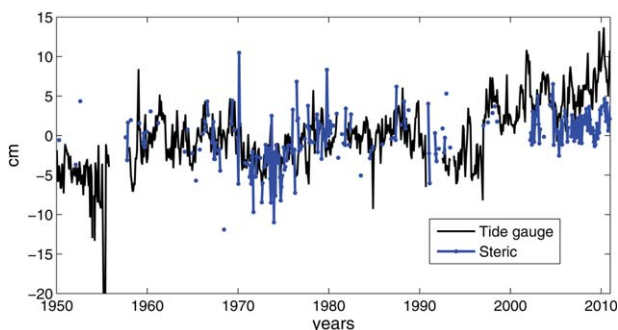


**Figure 10.** Observed monthly deseasoned atmospherically corrected sea level at the tide gauge (black) and steric sea level computed with a reference level of 500 m from individual profiles in the vicinity of Tenerife (blue).

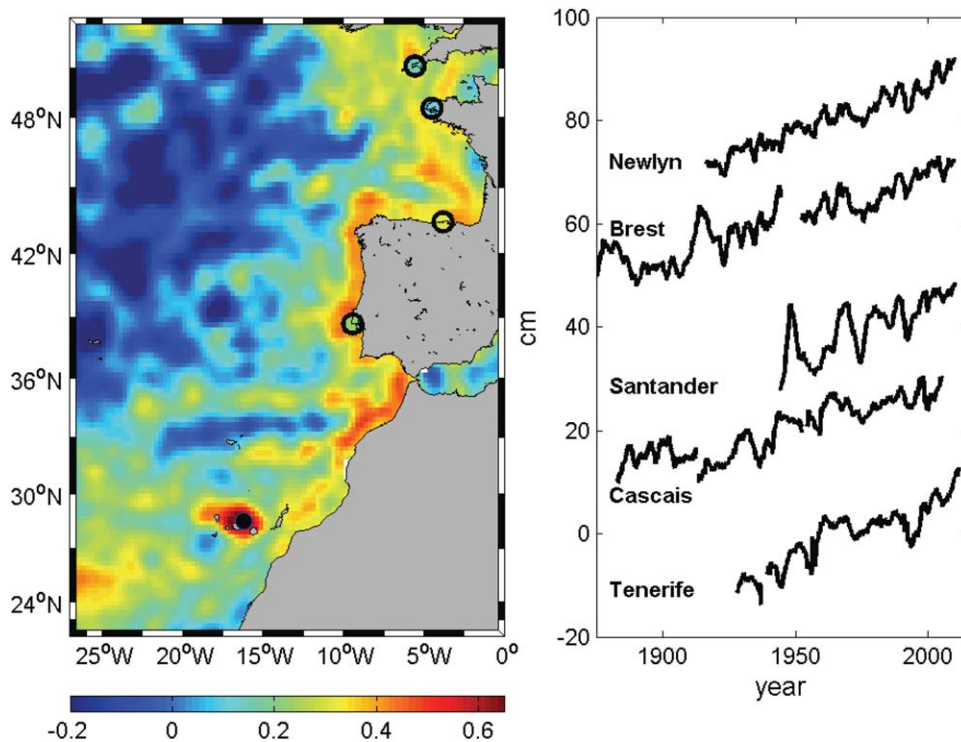


**Figure 11.** (left) Correlations between Tenerife time series and sea level anomalies from altimetry and other tide gauge records. Time series have been detrended and deseasoned. (right) Tide gauge records smoothed using 2 year running average. All time series were IB corrected, for consistency with altimetry.

by Calafat *et al.* [2012] at European tide gauges. Our results suggest that the coherency also holds at interannual time scales. As Tenerife is not located at the continental shore, the correlations in Figure 11 also suggest that the sea level signal generated over the shelf likely propagates through the open ocean in the form of Rossby waves.

[33] The relationship of sea level variability at Tenerife with large scale atmospheric forcing was explored. Provided that the influence of the atmospheric forcing occurs predominantly during winter, our analysis was restricted to this season. Maps of correlation between atmospherically corrected winter sea level at Tenerife and winter atmospheric pressure, wind stress, and wind stress curl over the North Atlantic are represented in Figure 12. Significant correlations up to 0.5 were found with winter wind stress curl over the center of action of the Azores High. Likewise, correlations were also high (reaching 0.5) with zonal and meridional wind stress and with atmospheric pressure over large regions of the North Atlantic. We must stress that the barotropic contribution of the atmospheric pressure and wind has already been removed from sea level observations. Therefore, the correlations suggest that sea level is related to steric variability driven by longshore winds which are in turn controlled by the large scale changes in the North Atlantic. Such large scale impact is also reflected in the relation of winter sea level at Tenerife and the winter NAO index (Figure 12, bottom) with a correlation of  $-0.56$ .

## 6. Discussion and Conclusions

[34] A new hourly sea level record starting in 1927 has been constructed using observations from five different tide

gauge records, all of them located at Santa Cruz harbor in Tenerife Island (North East Tropical Atlantic). An essential part of the analysis was the detailed study of the leveling surveys in the vicinity of the tide gauges, which guaranteed the stability of the benchmarks and ensured the consistency of the long time series. Only in this case, a new sea level record can be considered reliable and useful for climate studies.

[35] In the long term, it was found that the barotropic contribution did not have a relevant effect on long-term mean sea level changes at Tenerife. The linear trend was not significantly altered when this component was removed from the observations. However, it did account for 9% of the total monthly variance. At interannual scales, we demonstrated that sea level at Tenerife is largely driven by steric sea level changes of the nearby deep ocean. Our result is in agreement with Bingham and Hughes [2012] who showed that open ocean steric sea level is a good approximation to observed sea level at the coasts on eastern boundaries. In the same line, Williams and Hughes [2013] demonstrated, based on a numerical ocean model, that at the location of the Canary Islands sea level was coherent with fluctuations of steric height in the deep ocean.

[36] Sea level variations at Tenerife are linked with wind forcing along the continental coast that generates vertical movements of the thermocline which propagate poleward as a coastally trapped Kelvin wave. Such fluctuations imply changes of the thermohaline structure of the water column and thus steric variations [Calafat *et al.*, 2012]. It is remarkable that this signal was present at Tenerife despite being a few hundreds of kilometers off the continental

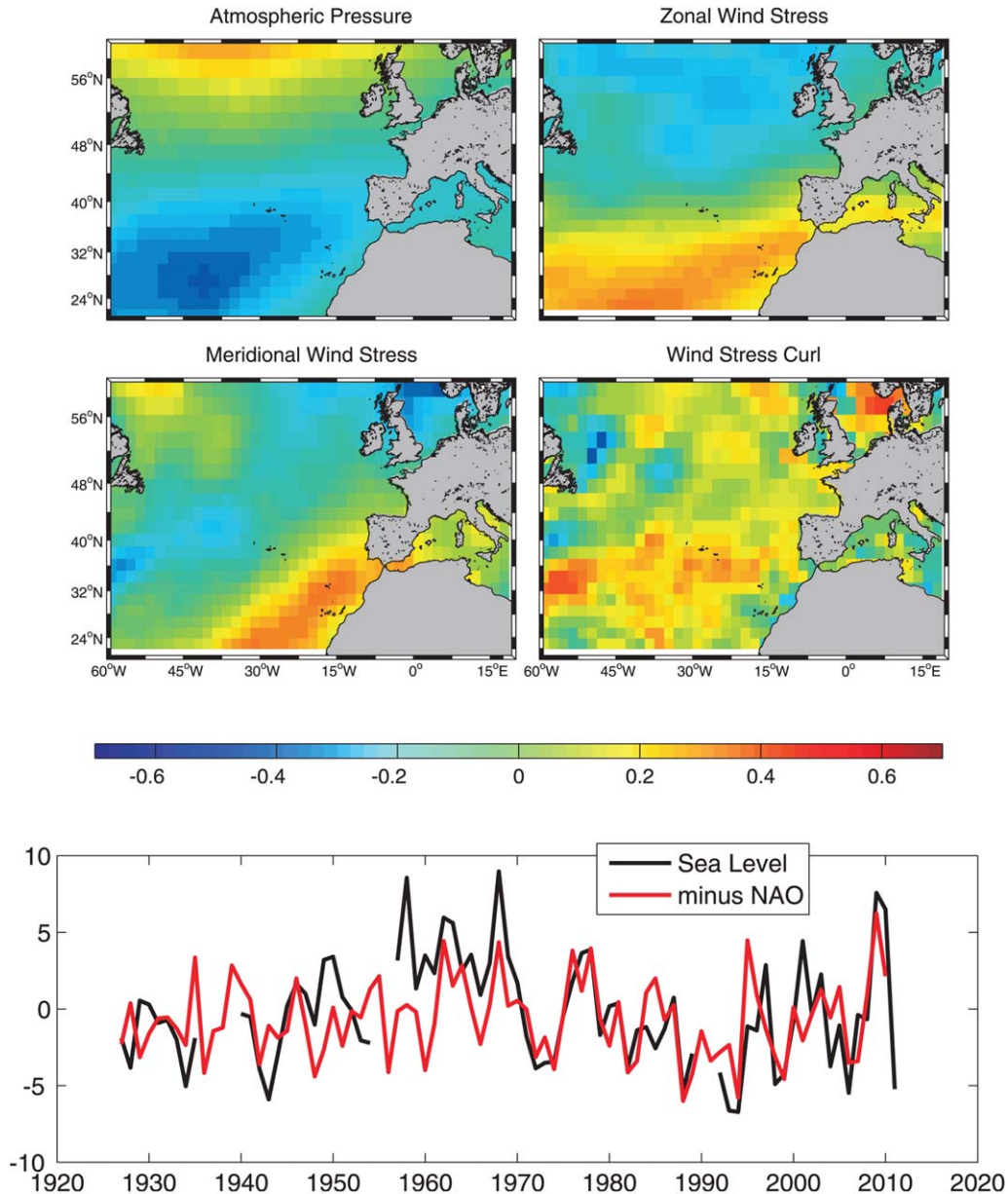


**Figure 12.** (top) Winter correlations between atmospherically corrected sea level at Tenerife and atmospheric variables. All time series have been detrended and deseasoned. (bottom) Winter sea level (black, in cm) and minus winter NAO (red, rescaled).

coast. Our findings therefore suggest that the waves generated by longshore winds may propagate from the eastern boundary through the open ocean to the western boundary as baroclinic Rossby waves, as proposed by *Miller and Douglas* [2007] and *Sturges and Douglas* [2011]. The coherent signal disappeared below 26°N, in agreement with *Calafat et al.* [2012], who reached the same conclusion but based on the output of a numerical model. This is the latitude where the Canary Current departs westward and separates from the coast.

[37] It is important to remark that, in order to estimate steric changes representative of the variability at Tenerife, we selected a relatively small area around the Canary Islands and used all the independent hydrographic profiles of T and S. When an interpolated product of T and S was

used instead (EN3 gridded monthly data), we did not find any correlation between observed and steric sea level, likely because the grid points of interpolated observations nearby Tenerife contained information from other noncoherent regions a few hundreds of km away.

[38] In summary, the analysis of the interannual and decadal sea level variability from the tide gauge record at Tenerife revealed that observed sea level is mostly of steric origin, which in turn is controlled by longshore winds linked to large scale atmospheric forcing. Large scale atmospheric patterns are also responsible of the strong upwelling along the African coast and the variability of the Canary Current. Therefore, it seems reasonable to suggest that there exists a relationship between the sea level variability observed at Tenerife and the transport of the Canary Current. The lack

of continuous and long-term observations of this transport prevents from quantifying such connection.

[39] Sea level has been rising at Tenerife at a (relative) rate of  $2.09 \pm 0.04$  mm/yr since 1927. This value is larger than the (geocentric) global average for the 20th century estimated in 1.7 mm/yr (Church and White, 2011). Glacial Isostatic Adjustment (GIA) models suggest stability of the site, with a value of 0.09 mm/yr [Peltier, 2004]. On the other hand, GPS observations date back to only 2009. The available solution for vertical velocities computed by *Santamaria-Gomez et al.* [2012] also suggests that the site to which the modern tide gauges are grounded is stable. Nevertheless, this finding has to be confirmed in the future as the available GPS position time series of 1.7 year long at Tenerife was too short for a robust GPS velocity estimate.

[40] Since 1950 onward, sea level rise was  $1.58 \pm 0.06$  mm/yr, from which only  $0.76 \pm 0.09$  mm/yr were attributed to steric sea level of the top 500 m. Differences between observed sea level and the steric contribution were larger during years 2000s. Whether the difference in trends is due to steric changes below 500 m or is attributed to other causes remains unclear.

[41] **Acknowledgments.** This work has been carried out in the framework of the projects VANIMEDAT-2 (CTM2009–10163-C02-01, funded by the Spanish Marine Science and Technology Program and the E-Plan of the Spanish Government) and ESCENARIOS (funded by the Spanish Agencia Estatal de Meteorología). M. Marcos acknowledges a “Ramon y Cajal” contract funded by the Spanish Ministry of Science. F. M. Calafat was supported by a Marie Curie International Outgoing Fellowship (IOF) within the 7th European Community Framework Programme (grant agreement number PEOF-GA-2010–275851). The Universitat de les Illes Balears provided a visiting professor grant for G. Wöppelmann. We thank Dr. Pedro Vélez for kindly providing quality controlled hydrographic data and the Spanish Port Authority for providing additional tide gauge observations. We are also grateful to the Spanish Geographical Institute for archiving the historical observations and to all tide gauge keepers and operators that for many years have managed and taken care of the different instruments and without whose dedication this work could never have been undertaken. The GPS data were obtained from SONEL ([www.sonel.org](http://www.sonel.org)).

## References

- Agnew, D. C. (1986), Detailed analysis of tide gauge data: A case history, *Mar. Geod.*, *10*, 231–255.
- Barbosa, S. M., M. E. Silva, and M. J. Fernandes (2008), Changing seasonality in the North Atlantic coastal sea level from the analysis of long tide gauge records, *Tellus, Ser. A*, *60*, 165–177.
- Bingham, R. J., and C. W. Hughes (2012), Local diagnostics to estimate density-induced sea level variations over topography and along coastlines, *J. Geophys. Res.*, *117*, C01013, doi:10.1029/2011JC007276.
- Calafat, F. M., D. P. Chambers, and M. N. Tsimplis (2012), Mechanisms of decadal sea level variability in the eastern North Atlantic and the Mediterranean Sea, *J. Geophys. Res.*, *117*, C09022, doi:10.1029/2012JC008285.
- Caldwell, P. (2012), Tide gauge data rescue, in *Proceedings of The Memory of the World in the Digital age: Digitization and Preservation*, edited by L. Duranti and E. Shaffer, Vancouver, British Columbia, Canada. [Available at [http://www.unesco.org/webworld/download/mow/mow\\_vancouver\\_proceedings\\_en.pdf](http://www.unesco.org/webworld/download/mow/mow_vancouver_proceedings_en.pdf).]
- Church, J. A., and N. J. A. White (2011), Sea-level rise from the late 19th to the early 21st Century, *Surv. Geophys.*, *32*, 585–602.
- Compo, G. P., et al. (2011), The twentieth century reanalysis project, *Q. J. R. Meteorol. Soc.*, *137*, 1–28.
- Dangendorf, S., C. Muddersbach, T. Wahl, and J. Jensen (2013), Characteristics of intra-, inter-annual and decadal sea-level variability and the role of meteorological forcing: The long record of Cuxhaven, *Ocean Dyn.*, *63*, 209–224, doi:10.1007/s10236-013-0598-0.
- Gill, A. E. (1982), *Atmosphere-Ocean Dynamics*, 662 pp., Academic, San Diego, Calif.
- Hernández-Guerra, A., et al. (2001), Temporal variability of mass transport of the Canary Current, *Deep Sea Res., Part II*, *49*(17), 3415–3426.
- Holgate, S., A. Matthews, P. L. Woodworth, L. J. Rickards, M. E. Tamisiea, E. Bradshaw, P. R. Foden, K. M. Gordon, S. Jevrejeva, and J. Pugh (2013), New data systems and products at the permanent service for mean sea level, *J. Coastal Res.*, *29*, 493–504.
- Ingleby, B., and M. Huddleston (2007), Quality control of ocean temperature and salinity profiles—Historical and real-time data, *J. Mar. Syst.*, *65*, 158–175, doi:10.1016/j.jmarsys.2005.11.019.
- Marcos, M., and M. N. Tsimplis (2007), Variations of the seasonal sea level cycle in southern Europe, *J. Geophys. Res.*, *112*, C12011, doi:10.1029/2006JC004049.
- Marcos, M., B. Puyol, G. Wöppelmann, C. Herrero, and M. J. Garcia-Fernandez (2011), The long sea level record at Cadiz (southern Spain) from 1880 to 2009, *J. Geophys. Res.*, *116*, C12003, doi:10.1029/2011JC007558.
- Miller, L., and B. C. Douglas (2007), Gyre-scale atmospheric pressure variations and their relation to 19th and 20th century sea level rise, *Geophys. Res. Lett.*, *34*, L16602, doi:10.1029/2007GL030862.
- Navarro-Pérez, E., and E. D. Barton (2001), Seasonal and interannual variability of the Canary Current, *Sci. Mar.*, *55*, 205–213.
- Pawlowicz, R., B. Beardsley, and S. Lentz (2002), Classical tidal harmonic analysis including error estimates in MATLAB using T\_TIDE, *Comput. Geosci.*, *28*, 929–937.
- Peltier, W. R. (2004), Global glacial isostasy and the surface of the ice-age earth: The ICE-5G (VM2) model and GRACE, *Ann. Rev. Earth Planet. Sci.*, *32*, 111–149.
- Pugh, D. T. (1987), *Tides, Surges and Mean Sea Level: A Handbook for Engineers and Scientists*, John Wiley, Chichester, U. K.
- Santamaría-Gómez, A., M. Gravelle, X. Collilieux, M. Guichard, B. Martín Míguez, P. Tiphaneau, G. Wöppelmann (2012), Mitigating the effects of vertical land motion in tide gauge records using a state-of-the-art GPS velocity field, *Glob. Planet. Change*, *98–99*, 6–17.
- Sturges, W., and B. C. Douglas (2011), Wind effects on estimates of sea level rise, *J. Geophys. Res.*, *116*, C06008, doi:10.1029/2010JC006492.
- Talke, S. A., and D. A. Jay (2013), Nineteenth century North American and Pacific tidal data: Lost or just forgotten?, *J. Coastal Res.*, in press.
- Testut, L., B. M. Míguez, G. Wöppelmann, P. Tiphaneau, N. Pouvreau, and M. Karpytchev (2010), Sea level at Saint Paul Island, southern Indian Ocean, from 1874 to the present, *J. Geophys. Res.*, *115*, C12028, doi:10.1029/2010JC006404.
- Volkov, D. L., G. Larnicol, and J. Dorandeu (2007), Improving the quality of satellite altimetry data over continental shelves, *J. Geophys. Res.*, *112*, C06020, doi:10.1029/2006JC003765.
- Watson, C., R. Burgette, P. Tregoning, N. White, J. Hunter, R. Coleman, R. Handsworth, and H. Brolsma (2010), Twentieth century constraints on sea level change and earthquake deformation at Macquarie Island, *Geophys. J. Int.*, *182*, 781–796, doi:10.1111/j.1365-246X.2010.04640.x.
- Wijffels, S., J. Willis, C. M. Domingues, P. Barker, N. J. White, A. Gronell, K. Ridgway, and J. A. Church (2008), Changing expendable bathythermograph fall rates and their impact on estimates of thermocline sea level rise, *J. Clim.*, *21*, 5657–5672, doi:10.1175/2008JCLI2290.
- Williams, J., and C. W. Hughes (2013), The coherence of small islands sea level with the wider ocean: A model study, *Ocean Sci.*, *9*, 111–119, doi:10.5194/os-9-111-2013.
- Woodworth, P. L., D. T. Pugh, and R. M. Bingley (2010), Long-term and recent changes in sea level in the Falkland Islands, *J. Geophys. Res.*, *115*, C09025, doi:10.1029/2010JC006113.
- Wöppelmann, G., N. Pouvreau, and B. Simon (2006), Brest sea level record: A time series construction back to the early eighteenth century, *Ocean Dyn.*, *56*, 487–497, doi:10.1007/s10236-005-0044-z.
- Wöppelmann, G., N. Pouvreau, A. Coulomb, B. Simon, and P. L. Woodworth (2008), Tide gauge datum continuity at Brest since 1711: France’s longest sea level record, *Geophys. Res. Lett.*, *35*, L22605, doi:10.1029/2008GL035783.